Development of a multi-level approach to model and optimise the Kalina Split Cycle for marine diesel engines

Ulrik Larsen, Tuong-Van Nguyen, Fredrik Haglind*

*Section of Thermal Energy, Department of Mechanical Engineering, Technical University of Denmark,
Building 403, Nils Koppels Allé, 2800 Kongens Lyngby, Denmark*

Abstract

In the marine sector there is a strong motivation for increasing the propulsion system energy efficiency, mainly because of increasing fuel prices and stricter upcoming emission regulations. The Kalina cycle, based on a mixture of ammonia and water as working fluid, exhibits higher conversion efficiencies than conventional power cycles and could be suitable for this purpose. The Split Cycle technique provides a method to further increase the thermal efficiency, by reducing the thermodynamic losses in the heat recovery system. This is achieved by having two separate streams of different ammonia concentrations entering and leaving a first evaporator stage before being mixed at the inlet of a second evaporator stage. It seems that modelling efforts showing the advantages of the Split Cycle have not been presented in the literature yet. Thus, a thermodynamic model of the Split Cycle is introduced in this work. Modelling and optimisation of the rather complex cycle requires approaching the problem at different system levels. This paper investigates tools and methods suitable for demonstrating the feasibility and advantages of the Split Cycle. The integrated model developed and presented in this paper combines three sub-models all using the NIST REFPROP equations of state: a separator and mixing subsystem model to handle the inherent constraints of the Split Cycle, a component-based model to optimise the heat exchanger operating conditions, and a process model to investigate the complete thermodynamic cycle. Results suggest a 9% net power output increase and 7% higher thermal efficiency compared to the baseline case.

Keywords: Kalina Split Cycle, Multi-Level Modelling, Process Integration, Waste Heat Recovery

1. Introduction

The International Maritime Organisation, under the United Nations organisation, is expected to adopt an energy efficiency design index (EEDI) for ships in 2013. For this reason and because of increasing fuel prices, this sector is in need of technologies that could further improve the efficiency of propulsion systems [1].

In this context, growing attention is paid to waste heat recovery power cycles, with the Kalina Cycle among those. Named from its inventor Alexander Kalina in 1983 [2], this thermodynamic cycle is using a mixture of water and ammonia as working fluid.

It was intended for waste heat recovery in three main fields of application: geothermics at temperatures from 100-200°C [3–10], integrated combustion engine heat recovery mainly at temperatures around 300°C [11–15] and for gas turbines at even higher temperatures [16–20]. A well-documented and tested Kalina cy-

---

*Principal corresponding author. Tel.: +4545254113
Email address: frh@mek.dtu.dk (Fredrik Haglind)

Nomenclature

Acronyms

EEDI   Energy Efficiency Design Index

EOS   Equation of State

IP   Intermediate Pressure

NIST   National Institute of Standards and Technologies

SC   Split Cycle

TRF   Tillner-Roth and Friend

Greek Symbols

Δ Difference between to states

Symbols

$\dot{m}$ Mass flow rate

H Non-specific enthalpy

h Specific enthalpy

p Pressure

Q Vapour quality

S Mass flow rate splitting fraction

T Temperature

x Ammonia fraction by mass

y Ammonia fraction by mole

Subscripts

b   Boiling point

c   Composite stream

d   Dew point

e   Exhaust gas

f   Separator feed stream

i   Inlet stream

l   Lean ammonia concentration

L   Liquid fraction

o   Outlet stream

r   Rich ammonia concentration

V   Vapour fraction

w   Working fluid

---

cle pilot plant converting heat at relatively high temperatures (450-550°C), from a gas furnace is the Canoga plant (USA)[4, 21–23].

In 1985 Kalina filed a petition for a US patent [24] on the Split Cycle, which is an alternative configuration of the Kalina process. In that petition the process is described only qualitatively and no model proving the comparative advantages seems to have been published since. The focus of this paper is therefore to present a thermodynamic model and an optimisation methodology of the Kalina Split Cycle process (SC).

In the conventional Kalina cycle, heat exchange in the heat recovery system only takes place between two streams: the heat source (e.g exhaust gases from a gas turbine) and the heat sink (ammonia-water mixture working fluid).

The specific feature of the SC is that two cold streams of different ammonia concentrations run through a preheater and a first evaporator stage. The two streams are then mixed before entering a second evaporator and a superheater.

The higher complexity of this process introduces additional degrees of freedom and unknowns at different system levels. There is therefore a need for a multi-level approach which addresses these modelling and optimisation challenges.

The approach and models developed to evaluate a Kalina SC are presented in the following. The thermodynamic performance of the modified heat recovery system is assessed in comparison with a baseline case, which is a conventional Kalina cycle based on exhaust gases

2

at 346°C from marine diesel engines, as documented by Bombarda [25]. The baseline case cycle is a type of Kalina cycle which is common in the literature, among others documented by Leibowitz et al. [21] and Jonsson et al. [19]. The SC model presented in the present work maintains the same constraints and boundary conditions as the baseline case.

2. Kalina Split cycle

Ammonia-water is a *zeotropic* mixture, which means that vapour and liquid phases at equilibrium never have both identical temperatures and compositions. During evaporation and condensation processes, the liquid and vapour compositions of zeotropic mixtures will continually change, and the saturation temperatures of these two phases will vary in consequence. It is thus possible to affect the thermophysical properties of the Kalina working fluid either by changing the operating pressure or by varying the ammonia concentration of the mixture.

Ammonia, being more volatile than water, is the first component to evaporate. The ammonia concentration in the liquid phase progressively decreases, causing a continual rise of the boiling temperature. The existence of this temperature glide may lead to a better match between the temperature profiles of the heat source and the working fluid, reducing the internal irreversibilities of the heat recovery process.

In an attempt to further reduce them, Dr. Kalina proposed in his patent petitions an alternative arrangement of this power cycle, referred to as the Split Cycle [24]. Other work of the same author [26] suggested that this configuration could reach a 2nd law efficiency of 75-80% for various heat sources.

The idea of the SC is to use two separate streams of ammonia-water, with different concentrations, running through a first evaporator. An important constraint proposed by Kalina is to have the ammonia-rich stream exit the first evaporator as saturated vapour (dew point) while the ammonia-lean stream exits as saturated liquid (bubble point). This proposed constraint is important for minimising thermodynamic losses and is therefore adopted in this work, leaving an investigation of the consequences of this assumption for future work. The constraint makes it harder to set initial parameters and to optimise the cycle and is thus providing motivation for developing the presented methodology. The two streams are then mixed into a composite stream and the newly formed two-phase mixture is evaporated and superheated before running through the turbine.

The modified Kalina SC is illustrated in Figure 1. The main differences from the conventional configuration are the use of additional mixers, splitters, pumps and recuperators between the separator and the turbine. In the simple Kalina cycle, the ammonia-rich vapour at the top outlet of the separator flows through a recuperator first and then a mixer before being condensed, while the ammonia-lean liquid at the bottom flows through another recuperator before being throttled.

In the SC, the very ammonia-rich vapour is first split into two sub-streams (19 and 26). Both are partly diluted in different proportions with fractions of the very ammonia-lean liquid flow and pass a succession of two recuperators where they are cooled down. The richer of these two streams (22) is then condensed (23) and pumped (24), before it is preheated (25) and flows through the heat recovery system. The leaner stream (29) is pumped (30) and preheated (31) before running through the first evaporator. These two streams are then mixed at the same temperature (1) before entering the second evaporator (2) and the superheater (3).

The very ammonia-lean liquid from the bottom of the separator is split into three sub-streams. Two (16 and 17) are used to adjust the concentration and mass flow rate of the
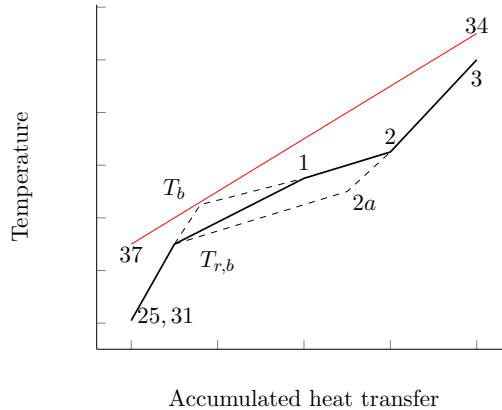
Figure 1: Process flowchart of the Kalina Split Cycle process

two rich vapour sub-streams from the top of the separator. The latter (13) runs through a recuperator where it is cooled down (14) before being throttled (15) and mixed with the ammonia-rich solution out of the turbine system.

Theoretical studies showed that, compared to the conventional configuration, the SC induces a lower entropy generation because of the better match between the temperature profiles of the two cold streams and the heat source [26]. The gradient of the evaporation temperature curve can to some degree be adjusted to the temperature profile of the heat source by selecting the optimal composition of each of the two streams, as illustrated in Figure 2. The line from (25,31) to the point $(T_{r,b})$ represent the preheating stage. From here to point (1), (2) and (3) the fully drawn line shows the heat transfer in the SC case. The upper dashed line show how the heat transfer would be if the stream were not split but instead the compos-

ite stream was used. The point (T_b) shows the boiling point of the composite stream, and it is clear that the pinch point temperature difference is much smaller and possibly violated in this case. The lower dashed line from $(T_{r,bub})$ to (2), shows how the heat transfer would happen if only the rich stream concentration was used. Evaporation would occur at lower temperatures and thus likely causing a lower thermal efficiency.

3. Methodology

Given the constraint of having identical temperatures and pressures of the rich and lean streams exiting the first evaporator, whilst also requiring the rich stream to be saturated vapour and the lean stream saturated liquid, initial parameter estimation and subsequent optimisation at full process level are not feasible. The choice was made to build two sub-models which could accurately predict the op-

Figure 2: Theoretical T-Q diagram of the Heat Recovery System to explain the Split Cycle

timum performance of the full process and subsequently obtain full process validation. In the next sub-sections, three modelling levels are considered and presented: thermodynamic property level, governing subsystems at component level and full process level.

3.1. Thermodynamic property level

Tillner-Roth and Friend (TRF) presented their model of the ammonia-water system in 1998 [27]. Their motivation was the rising interest in modelling the Kalina cycle and thus the arising need for an accurate model for this working fluid mixture over a wide range of concentrations, temperatures and pressures. At the time, there was seemingly no model covering both the liquid, two-phase and vapour domains with satisfying accuracy [27]. Based on a thorough survey [28] of the publicly available experimentally obtained properties for the system, a fundamental equation of state (EOS) which is claimed to be accurate up to 40 MPa was derived.

Thorin et al. [29] compared in 1999 the Tillner-Roth and Friend model with both experimental data and two other EOS derived for the ammonia-water system (Stecco-Desideri and Ibrahim and Klein). Analysis showed that the TRF EOS is generally more accurate than the two other EOS because of an additional correction factor. Additionally the TRF EOS

is valid up to higher pressures than the two others which are valid up to 11.5 and 20 MPa respectively. Thorin also compared the thermal efficiency of a Kalina cycle using boiler pressures between 10-18 MPa and found that the choice of EOS does influence the efficiency up to 1.5% points at high pressures.

For the above mentioned reasons and since the TRF EOS is included as a property model in Aspen and in Matlab with NIST REFPROP, this EOS was chosen for the sub- and full process models. A disadvantage of using this property model is its complexity. Except when the phase is specified, the model needs first to determine if the fluid is in the liquid, vapour or two-phase domain. As experienced by the authors and as also confirmed by personal communication with Eric Lemmon (NIST), the TRF model in REFPROP has occasional non-convergence issues (at certain random points in the thermodynamic domain). In Aspen Plus it is possible to specify phase and thereby to increase the convergence efficiency. When compared to the Peng-Robinson EOS, the TRF EOS seems to be significantly more accurate for the Kalina cycle. Consequently, the baseline model in the present work has minor deviances in the thermodynamic properties at some points in the process, compared to the model in the work of Bombarda (which is used as baseline) [25]. An advantage of the Peng-

Robinson EOS is that it is simpler and converges easily, a benefit traded in this work in order to obtain better accuracy.

3.2. Subsystem Level

A subsystem is here regarded as a system of components which is an integrated part of the whole process. In the following, two subsystems are discussed: firstly, the heat exchangers system described earlier, and secondly, the separation and mixing system. The motivation for making the models of these subsystems is to ease initial parameter estimations and optimisation of the process. Both subsystems were validated using corresponding subsystem models in Aspen Plus.

3.2.1. Heat exchanger system

The composite working fluid mass flow rate exiting the boiler can be used as a measure proportional to the process work output, since the thermodynamics state at the boiler outlet is held constant. The aim of the following methodology is thus to uncover the relation between the maximum possible mass flow rate and the composition of the two split streams.

Rich and lean streams entering and exiting the first evaporator should have identical temperatures and pressures, and leave as saturated vapour and liquid respectively. Any chosen composition of the rich stream (x_r) results therefore in only one possible composition of the lean one and only one ratio between the rich and lean mass flow rates.

Thus the final optimisation is based on the rich stream composition versus boiler mass flow.

Composition of the lean mass flow (x_l) is calculated from the rich stream composition by solving the following equation system:

$$T_{r,d} = T(p = p_w, Q = 1, x = x_r) \qquad (1)$$
$$T_{l,b} = T(p = p_w, Q = 0, x = x_l) \qquad (2)$$
$$T_{r,d} - T_{l,b} = 0 \qquad (3)$$

where $T_{r,d}$ is the dew point temperature of the rich stream, $T_{l,b}$ is the bubble point temperature of the lean stream, p_w is the working fluid pressure and Q is vapour quality. Then, the mass flow ratio between the rich and lean streams are found by solving the following mass balance equations (note that the actual mass flow of the composite stream $(\dot{m}_c)$ is not known at this stage):

$$\dot{m}_c - \dot{m}_r + \dot{m}_l = 0 \qquad (4)$$
$$x_c\dot{m}_c - x_r\dot{m}_r - x_l\dot{m}_l = 0 \qquad (5)$$

where $\dot{m}_r$ and $\dot{m}_l$ are the mass flow rates of the rich and lean streams and x_c is the composite stream composition, i.e. the stream exiting the boiler. Using an energy balance over the entire boiler, the mass flow of the (composite) working fluid, can be found. The hot source mass flow, pressure and temperature at the outlet and inlet are known parameters. Also known is the superheater approach, the pressure of the working fluid as well as the inlet states (pressure, temperature and composition) of the working fluid streams:

$$\dot{m}_c = \dot{m}_e \frac{h_{e,i} - h_{e,o}}{h_{w,o} - \frac{\dot{m}_r}{\dot{m}_r + \dot{m}_l}h_{r,i} - \frac{\dot{m}_l}{\dot{m}_r + \dot{m}_l}h_{l,i}} \qquad (6)$$

where $\dot{m}_e$, $h_{e,i}$ and $h_{e,o}$ are the mass flow rate and enthalpies in and out of the boiler respectively. $h_{w,o}$, $h_{r,i}$ and $h_{l,i}$ are the enthalpies of the working fluid exiting the boiler and the rich and lean stream entering. All enthalpies in the above equation are found using $h = h(T, p, x)$. Upon finding the mass flow of the composite stream, the rich and lean mass flows can be calculated. In order to estimate the minimum temperature difference in the boiler, both heat exchangers are divided into a number of steps (n). The first evaporator (including preheater) is modelled by dividing the temperature between outlet and inlet into steps ΔT_s and assuming temperature equilibrium between the

lean and rich streams in each division. Hereby the enthalpy in each step is found:

$$\Delta T_s = \frac{(T_{l,b} - T_{w,i})}{n} \tag{7}$$

$$T_{r,i} = T_{l,i} = T_{w,i} + (i-1)\Delta T_s \tag{8}$$

$$\Delta H_{s,j} = \dot{m}_r(h_{r,j} - h_{r,1}) + \dot{m}_l(h_{l,j} - h_{l,1}) \tag{9}$$

where $i = [2, 3, ...(n+1)]$ and $j = [2, 3, ...n]$, $T_{w,i}$ is the working fluid temperature, ΔH_s the difference in enthalpy between two steps with i and j representing the step number. Since the enthalpy increase numerically in each step is the same for working fluid and heat source, the temperature of the hot source at each step is thus found from the enthalpies, $T = T(h, p, x)$. The minimum temperature difference can now be found and a similar approach is used for the second evaporator. By varying x_r the maximum working fluid mass flow rate is found, but still the question remains whether the mixing system can deliver the corresponding rich and lean streams.

3.2.2. Mixing system

Desired outputs from the mixing system model are the mass flow fractions of the three splitters (S_1, S_2 and S_3 respectively), as shown in figure 1, and the mass flow feeding the separator ($\dot{m}_f$). Inputs are the mass flow rates and compositions found in the heat exchanger subsystem model. Being fed by the separator, the mixing subsystem model includes this component beginning from the inlet of the separator, a stream which composition (x_f) is chosen to be the same as the baseline case for comparison reasons. Other inputs to the model are p_w, x_c and $\dot{m}_c$. Assuming an isothermal adiabatic process, the single stage separator can be modelled with the use of the EOS and an ammonia mass balance. The equilibrium concentrations of the liquid and vapour phases (x_l and x_v) are found using a REFPROP function, provided an assumed temperature and pressure

(T_f and p_f) similar to the baseline case (from the Bombarda article [25]):

$$[x_L, x_V] = X(T = T_f, p = p_f, x = x_f) \tag{10}$$

where $x_{18} = x_V$ and $x_{11} = x_L$ (figure 1). Solving the following equation system of mass balances, provides the liquid and vapour mass flows from the separator:

$$\dot{m}_{11} = \dot{m}_f - \dot{m}_{18} \tag{11}$$

$$x_f \dot{m}_f - x_{18} \dot{m}_{18} - x_{11} \dot{m}_{11} = 0 \tag{12}$$

The following equations are common for the three splitters, here splitter 1:

$$x_{26} = x_{18} \tag{13}$$

$$x_{19} = x_{18} \tag{14}$$

$$\dot{m}_{26} + \dot{m}_{19} = \dot{m}_{18} \tag{15}$$

$$\dot{m}_{26} = S_1 \dot{m}_{18} \tag{16}$$

Where S_1 is the ratio to be found and used in the full process model. The mixers are described by both a mass balance and an ammonia mass balance:

$$\dot{m}_{27} = \dot{m}_{16} + \dot{m}_{26} \tag{17}$$

$$x_{27} \dot{m}_{27} = x_{16} \dot{m}_{16} + x_{26} \dot{m}_{26} \tag{18}$$

This equation system is solved iteratively and returns the separator feed mass flow and the splitter fractions, thereby producing the desired rich and lean streams characteristics ($\dot{m}, x$). Coupling of the two sub models described here provides an accurate tool needed to optimise the full process of the Kalina Split cycle within the boundary conditions given.

3.3. Process modelling
3.3.1. Available models

Aspen Plus is a widely used commercial process simulation software, which is based on several methods and packages for estimations of

thermodynamic properties. Modelling of the overall Kalina cycle was carried out using Aspen Plus(R) v7.2, based on the REFPROP property method for consistency.

This process flow-sheet program also includes several sets of modules for simulating unit operations such as compressors and turbines, heat exchangers and separators, pumps and throttles, etc. Calculations are based on physical relations (mass and energy balances, heat transfer and fluid dynamics) and are conducted iteratively.

Aspen Plus is a sequential modular program, meaning that the sets of equations used to model the overall system are solved in a certain order, in contrast to equation-oriented programs which solve the equation sets simultaneously. In case of processes with internal loops (e.g thermodynamic cycles), equation sets are solved iteratively and the implementation of initial guess values and constraints is needed to avoid convergence issues and accelerate the problem resolution.

It is possible to implement kinetic-rate models (e.g kinetic mechanisms for chemical reactions and rate-based models for separation and distillation). However, it is assumed that an equilibrium-based separator module can rigorously model the two-phase separator used in Kalina cycles.

3.3.2. General modelling assumptions

The simulations of the simple Kalina cycle and of the Split Cycle were both based on the following assumptions and data, adopted from the baseline case, which is based on work presented by Bombarda [25]. The chemical compounds considered in the simulations are: N_2, O_2, H_2O, CO_2, Ar and NH_3. The heat source considered in this study are exhaust gases from two marine diesel engines, with the following molar composition 74.6% N_2, 11.7% O_2, 6.7% H_2O, 5.9% CO_2 and 1.1% Ar and a total mass flow rate of $35\frac{kg}{s}$. The ammonia-water mixture enters the heat recovery system at a temperature of 83.5°C and has the following mass com-

position at the inlet of the turbine 77.2% NH_3, 22.8% H_2O. Assumptions on the process design are listed below:

- Exhaust gas pressure and temperature: 2 bar and 346°C

- Stack temperature: 127.7°C

- Minimum allowable pinch point temperature difference in boiler: 21.9°C

- Super heater approach: 16°C

- Minimum allowable pinch point temperature difference in low and intermediate pressure (IP) recuperators: 4.5°C

- Minimum allowable pinch point temperature difference in high pressure recuperator: 16.5°C

- Pressure levels: 5.94, 10, 100 bar

- Separator temperature: 100°C

- Cooling water temperature: 20°C

- Adiabatic separator

- Homogeneous fluid flow and temperatures

- Turbine mechanical and isentropic efficiency: 96% and 75%

- Pumps driver efficiency and isentropic efficiency: 95 % and 70%

- Ammonia concentration in composite stream, y_3: 78.6%

- Heat to the environment and pressure losses in heat exchangers are neglected

3.3.3. Specific modelling assumptions

Specific assumptions related to the design of the Kalina process without Split Cycle are listed below:

- IP condensation temperature: 33°C

- IP recuperator: 2 streams

Specific assumptions related to the design of the Kalina process with Split Cycle are listed below:

- Additional pumps have the same efficiency

- Additional mixers and splitters are adiabatic

- IP condensation temperature: 26°C

- IP recuperator: 4 streams

One of the main differences between the conventional Kalina process and the Split Cycle is the ammonia concentration of the rich mixture at the inlet of the heat recovery system. In the first case, the ammonia content is between 70-75%$_{wt}$, which corresponds to a condensing temperature of about 33°C at a pressure of 10 bar. In the second case, the ammonia content of the rich stream is 10 percentage points higher, which corresponds to a condensing temperature of 26°C.

In order to fully condense the ammonia-rich stream in the Split Cycle, the operating temperature of the condenser should be decreased from 33°C to 26°C (effectuated by larger cooling water flow rate). As a consequence, the operating parameters of the cooling system and of the condenser are slightly different compared to the baseline case.

3.3.4. Optimisation

Optimisation of the Split Cycle is conducted by changing the pressure level to reach the same pinch point temperature difference in the heat recovery system (21.9°C) while keeping the same temperature inlet and outlet conditions, and an identical ammonia concentration at the boiler outlet (point 3 Figure 1).

4. Results and discussion

By varying the rich (and lean) stream compositions, the temperatures of the working fluid in the first evaporator changes and thus also the pinch point. This variation is shown in Figure 3 at pressures from 100 to 140 bar. The constraint of pinch point temperature difference of 21.9°C is not respected at any concentration at 140 bar pressure and above and the maximum net work output without any violation is found at 138 bar and an x_{rich} of 0.90. It is also shown in the figure how the pinch point temperature difference is larger than the baseline case of 21.9°C, when using SC at baseline pressures and high rich stream concentrations.
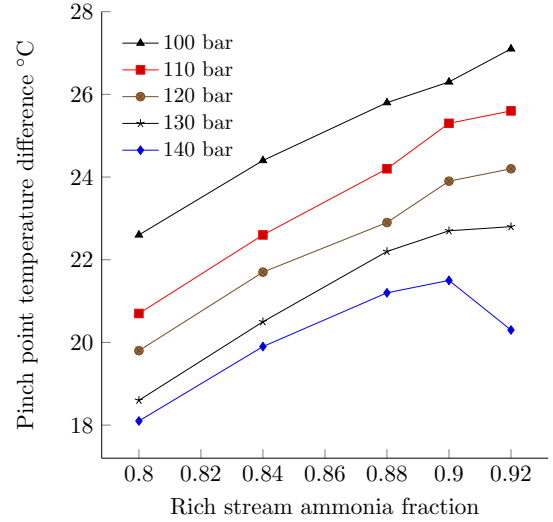
Figure 3: Rich stream composition versus pinch point temperature difference

Changing the rich and lean streams compositions does not enable significant changes in the maximum mass flow rate and consequently the turbine work output. The maximum obtainable turbine work output at various concentrations and pressures is shown in Figure 4. The maximum output is, in most cases, found at rich stream compositions of about 0.90.
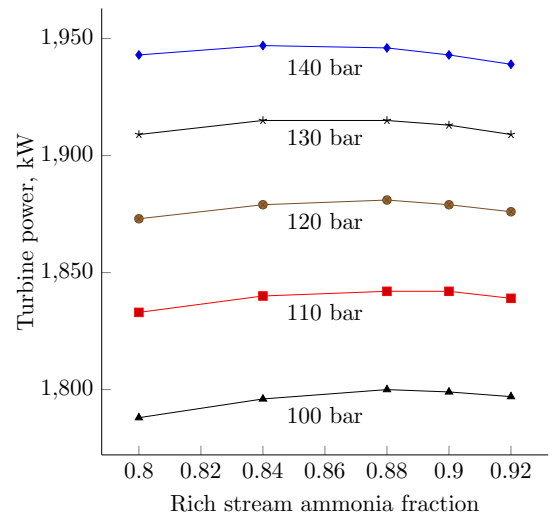
Figure 4: Rich stream composition versus turbine power

In Figure 5 the temperatures as a function of the accumulated heat transfer in the entire heat

recovery system, as seen from the hot source side, is shown. Looking at the SC case at 100 bar, it is seen that the alignment of temperatures of the hot and cold streams, is deteriorated compared to the baseline case. Despite that, the turbine work output is slightly higher because the early evaporation of the rich stream enables a higher mass flow rate, a parameter limited by the pinch point temperature difference. Compared to the baseline case, the optimised case at 138 bar shows a visibly closer alignment of temperatures of the hot and cold streams, while the pinch point temperature difference is not changed from that of the baseline case. The average temperature in the heat uptake is clearly higher in this case. Although the Split Cycle streams are only separated in the first evaporator, the improved match continues through the second evaporator.
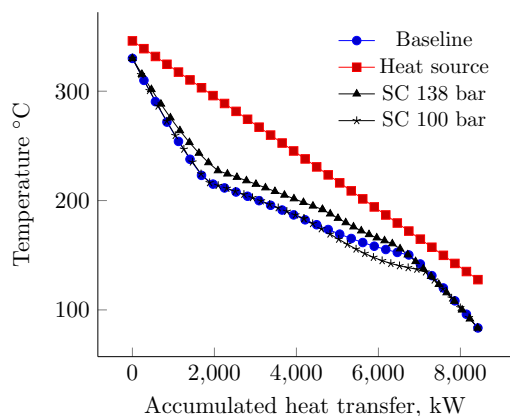

Figure 5: T-Q diagram of the boiler

Using the SC configuration is thus seen to enable an increased maximum pressure in the cycle without violating the pinch point temperature difference constraint. Reversely, the baseline case does not allow higher pressures without a pinch point temperature difference violation, indicating that the baseline cycle parameters are indeed optimised. Figure 6 shows how the turbine work, cycle net work and thermal efficiency increase with higher boiler pressure. The shown cases were optimised in terms of concentrations and mass flows of the rich and lean streams, aiming at maximum power. Even more power could be obtained with a smaller pinch point temperature difference. Temperature and vapour quality at the turbine outlet decrease slightly as the inlet pressure increases without affecting the rest of the process markedly. The vapour quality at 138 bar is 96% compared to 99% in the baseline case.
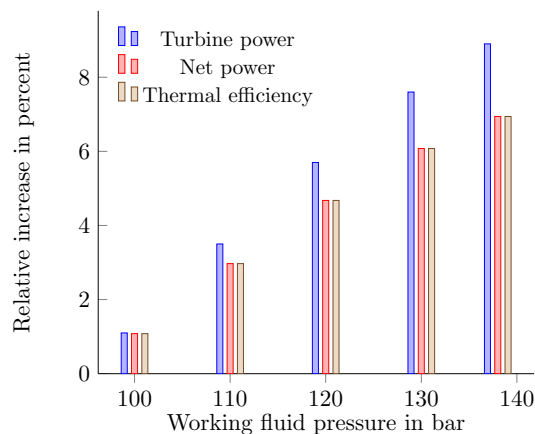

Figure 6: Cycle output versus maximum pressure

As should be expected, the relative increases in thermal efficiency of the cycle and the net work output are identical and in the baseline case the thermal efficiency is 20.1% while at 138 bar in the optimised SC case 21.5 % is achieved. States of all the points in the optimised Split Cycle are shown in the appendix.

5. Conclusion

A thermodynamic model of the Kalina Split Cycle and a methodology for optimising the cycle was presented. The methodology, consisting of two subsystem models, has made it possible to optimise the entire cycle effectively. It has been shown that the concept of using two different streams instead of one running through the evaporator does bring some advantages. The temperature development of the working fluid can be altered by changing the composition and mass flow rates of the two streams, in order to obtain a better alignment

of temperatures of the hot and cold streams in the heat exchanger.

Since the richer stream evaporates first and thus results in a larger pinch point temperature difference, higher boiler pressures and work outputs are enabled without violating the pinch point temperature difference limitation.

Results suggest a turbine power output increase of about 9% can be achieved resulting in an increase in thermal efficiency of 7%, or an increase from 20.1 to 21.5% thermal efficiency for the cycle.

Acknowledgements

References

[1] The International Maritime Organisation, IMO . The International Maritime Organisation. 2012.

[2] Kalina A. Combined cycle and waste heat recovery power systems based on a novel thermodynamic energy cycle utilizing low-temperature heat for power generation. Am Soc Mech Eng, (Pap); (United States) 1983;83-JPGC-GT.

[3] Kalina A, Leibowitz H, Lazzeri L, Diotti F. Recent development in the application of Kalina cycle for geothermal plants, geothermal-energy.org. 1995.

[4] Lazzeri L, Diotti F, Bruzzone M, Scala M. Application of Kalina Cycle to Geothermal Applications. Proceedings of the American Power Conference 1995;57(V1):370–3.

[5] Madhawa Hettiarachchi HD, Golubovic M, Worek WM, Ikegami Y. The Performance of the Kalina Cycle System 11(KCS-11) With Low-Temperature Heat Sources. Journal of Energy Resources Technology 2007;129(3):243–.

[6] Koroneos CJ, Rovas DC. Electricity from Geothermal Energy with the Kalina Cycle An Exergy Approach. In: International Conference on Clean Electrical Power, 2007. ICCEP '07. 2007, p. 423–8.

[7] Kalina AI. Application of recent developments in Kalina Cycle technology to the utilization of high temperature geothermal sources. Transactions - Geothermal Resources Council 2008;32:346–50.

[8] Nasruddin D, Usvika R, Rifaldi M, Noor A. Energy and exergy analysis of kalina cycle system (KCS) 34 with mass fraction ammonia-water mixture variation. Journal of Mechanical Science and Technology 2009;23(7):1871–6.

[9] Ogriseck S. Integration of Kalina cycle in a combined heat and power plant, a case study. Applied Thermal Engineering 2009;29(14-15):2843–8.

[10] Valdimarsson P. Geothermal power plant cycles and main components. Tech. Rep.; University of Iceland; Reykjavik; 2011.

[11] Jonnson M, Thorin E, Svedberg G. Gas Engine Bottoming Cycles With Ammonia-Water Mixtures as Working Fluid. ASME -Publications- PWR 1999;34(NO 2):55–66.

[12] Jonsson M, Yan J. Exergy and Pinch Analysis of Diesel Engine Bottoming Cycles with Ammonia-Water Mixtures as Working Fluid 2000;3(2):57–71.

[13] Jonsson M, Yan J. Ammonia-water bottoming cycles: a comparison between gas engines and gas diesel engines as prime movers. Energy 2001;26(1):31–44.

[14] Xia B, Tanaka S, Nakazawa T, Sugita H. Research on the application of the combined cycle used in the power plant for ship propelling systems. Proceedings of the International Conference on Power Engineering : ICOPE 2003;2003(3):3–162.

[15] He M, Zhang X, Zeng K, Gao K. A combined thermodynamic cycle used for waste heat recovery of internal combustion engine. Energy 2011;36(12):6821–9.

[16] Marston CH. Parametric Analysis of the Kalina Cycle. Journal of Engineering for Gas Turbines and Power 1990;112(1):107–.

[17] Marston CH, Hyre M. Gas Turbine Bottoming Cycles: Triple-Pressure Steam Versus Kalina. Journal of Engineering for Gas Turbines and Power 1995;117(1):10–.

[18] Nag P, Gupta A. Exergy analysis of the Kalina cycle. Applied Thermal Engineering 1998;18(6):427–39.

[19] Jonsson M, Yan J. Gas turbine with Kalina bottoming cycle versus evaporative gas turbine cycle. In: Proceedings of the International Joint Power Generation Conference. New Orleans: ISSN 1537-6753; 2001, p. 77–85.

[20] Zhang Y, He M, Jia Z, Liu X. First law-based thermodynamic analysis on Kalina cycle. Frontiers of Energy and Power Engineering in China 2008;2(2):145–51.

[21] Leibowitz HM, Zervos N. Installation and Early Test Results of a 3 MW Kalina Cycle Demonstration Plant. SAE International 1992;1992-08-03.

[22] Zervos NG, Leibowitz HM, Robinson K.

Innovative Kalina cycle promises high efficiency [combined cycle power stations]. Power 1992;136(4):177–9.

[23] Zervos NG, Leibowitz HM, Robinson K. Startup and operating experience of the Kalina cycle demonstration plant. American Society of Mechanical Engineers, International Gas Turbine Institute (Publication) IGTI 1992;7.

[24] Kalina A. Website of Rex Research, US Patent # 4,548,043. 1985.

[25] Bombarda P, Invernizzi CM, Pietra C. Heat recovery from Diesel engines: A thermodynamic comparison between Kalina and ORC cycles. Applied Thermal Engineering 2010;30(2-3):212–9.

[26] Kalina A. A Kalina cycle technology and its applications. In: American Institute of Chemical Engineers, New York, NY. American Institute of Chemical Engineers, New York, NY; 1986, p. 1–13.

[27] Tillner-Roth R, Friend D. A Helmholtz free energy formulation of the thermodynamic properties of the mixture {water+ammonia}. Journal of Physical and Chemical Reference Data 1998;27(1):63–96.

[28] Tillner-Roth R, Friend DG. Survey and Assessment of Available Measurements on Thermodynamic Properties of the Mixture {Water + Ammonia}. Journal of physical and chemical reference data 1998;27(1):45–62.

[29] Thorin E. Comparison of Correlations for Predicting Thermodynamic Properties of AmmoniaWater Mixtures. International Journal of Thermophysics 2000;21(4):853–70.

Appendix A. States in the Kalina Split Cycle referring to Figure 1

Point	p, bar	T, $°C$	x	$\dot{m}$, $\frac{kg}{s}$	Q
1	138.0	191.8	0.772	4.48	0.458
2	138.0	227.9	0.772	4.48	1.000
3	138.0	330.0	0.772	4.48	-
4	5.9	108.7	0.772	4.48	0.958
5	5.9	75.7	0.772	4.48	0.713
6	5.9	73.0	0.600	7.14	0.426
7	5.9	25.0	0.600	7.14	0.000
8	10.0	25.1	0.600	7.14	-
9	10.0	75.0	0.600	7.14	0.316
10	10.0	100.0	0.600	7.14	0.479
11	10.0	100.0	0.308	3.78	0.000
12	10.0	100.0	0.308	2.76	0.000
13	10.0	100.0	0.308	2.65	0.000
14	10.0	44.0	0.308	2.65	0.000
15	5.9	44.1	0.308	2.65	-
16	10.0	100.0	0.308	1.02	0.000
17	10.0	100.0	0.308	0.11	0.000
18	10.0	100.0	0.928	3.35	1.000
19	10.0	100.0	0.928	1.93	1.000
20	10.0	100.0	0.895	2.04	0.948
21	10.0	75.0	0.895	2.04	0.848
22	10.0	29.9	0.895	2.04	0.248
23	10.0	26.0	0.895	2.04	0.000
24	138.0	30.4	0.895	2.04	-
25	138.0	83.5	0.895	2.04	-
26	10.0	100.0	0.928	1.42	1.000
27	10.0	100.0	0.669	2.44	0.590
28	10.0	83.3	0.669	2.44	0.493
29	10.0	35.0	0.669	2.44	-
30	138.0	38.2	0.669	2.44	-
31	138.0	83.5	0.669	2.44	-
32	138.0	191.8	0.669	2.44	0.000
33	138.0	191.8	0.895	2.04	1.000
34	2.0	346.0	-	35.00	-
35	2.0	254.8	-	35.00	-
36	2.0	227.1	-	35.00	-
37	2.0	127.8	-	35.00	-